# Design and Optimization of a Spectrometer for High-Resolution SD-OCT

**Lulu Wang[1], Xiaojun Yu[2], Xin Ge[1], Xuan Wu[1], Xianghong Wang[1], En Bo[1], Nanshuo Wang[1], Xinyu Liu[1], Guangming Ni[3], and Linbo Liu[1,*]**

[1]School of Electrical and Electronic Engineering, Nanyang Technological University, Singapore, 639798

[2]School of Automation, Northwestern Polytechnical University, Xi'an, Shaanxi, China, 710072

[2]School of Optoelectronic Information, University of Electronic Science and Technology of China, Chengdu, Sichuan, China, 610054

E-mail: LIULINBO@ntu.edu.sg

5 November 2018

**Abstract.** We report the design of a high-efficiency spectrometer for high-resolution spectral-domain optical coherence tomography (SD-OCT). The advantages of the proposed spectrometer are two-fold: first, we use a concave mirror instead of a camera lens (as typically used) as the focusing optics to both improve the transmission efficiency and eliminate chromatic aberrations; second, the new design involves a much lower cost than a spectrometer based on refractive optics. Both theoretical analyses and imaging experiments were conducted to characterize and validate the performance of the proposed spectrometer. Compared with a typical refractive optics-based spectrometer, the proposed spectrometer is approximately 1.27 times more efficient, has a comparable ranging depth and maintains a high axial resolution.

PACS numbers: 42.15.Eq, 42.62.Be, 87.85.Ox, 87.85.Pq

*Keywords*: Optical Coherence Tomography, Imaging systems, Medical and biological imaging, Medical optics instrumentation. Submitted to: *Laser Phys. Lett.*

## 1. Introduction

Spectral-domain optical coherence tomography (SD-OCT) has been established as a diagnostic imaging tool over the past few decades due to its advantages of high sensitivity and speed [1–7]. With the advent of broadband light source technologies, studies have pushed the axial resolution to 1-2 $\mu m$ [5, 8, 9], which has enabled visualization of cellular and subcellular structures. However, the increased spectral bandwidth presents new challenges for spectrometer design. In addition, a compelling demand has to be met to lower the cost of devices, which is a major roadblock towards the successful clinical application of ultrahigh resolution OCT (UHR OCT) and Micro-OCT [10–13]. Currently, spectrometers typically utilize refractive optical components, i.e., achromatic lenses, to collimate the interference signal from the detection fiber to a diffraction grating followed by focusing of the angularly dispersed spectrum onto a line-scan camera using a refractive camera lens [14]. A customized Cooke triplet lens [15], multi-element scan lens, camera, and commercially available photography lenses have all been used for the camera lens [16, 17]. The currently available refractive optics may be associated with the following issues to support the ultrahigh resolution and low-cost applications. First, the use of an achromatic lens as the collimation lens does not usually eliminate all of the chromatic aberrations and is also costly compared to reflective lenses. Secondly, most of the commercial camera lenses employed in spectrometer designs suffer significant losses in the near-infrared (NIR) wavelength range as they were specifically designed for visible light [17, 18]. It was proposed that replacing the refractive camera lens with reflective one helps elimination chromatic aberrations [19]. However, to the best of our knowledge, few studies fully characterize all-a reflective optics-based spectrometer for ultrahigh resolution applications.

We report an all-reflective-optics based spectrometer design to both to improve transmission efficiency and eliminate chromatic aberrations. In this study, we firstly used Zemax software to design reflective optics according to a typical ultrahigh resolution design input. We secondly fabricated an all-reflective-optics based spectrometer and conducted experiments to characterize the performances of the proposed design, and the results were compared with those obtained using a typical refractive-optics based spectrometer.

## 2. Method

The design input of the proposed all-reflective-optics spectrometer has a center wavelength of 845 nm and 170 nm spectral bandwidth (3dB). The input fiber was Nufern 780-HP with a nominal numerical aperture (NA) of 0.13 at 1% intensity, and the linear camera AViiVA EM4, e2V, Chelmsford, UK) had a pixel size of 14 $\times$ 28 $\mu$m (width $\times$ height) and array size of 2048. The objective of the design was to achieve improved spectrometer efficiency, ranging depth, and axial resolution with respective to the corresponding all-refractive-optics spectrometer. The spectrometer efficiency can be

calculated by the equation (1):

$$\eta = \frac{F_{WC} \cdot R_i}{(\frac{S_{pr}}{2^{b_t}} \cdot F_{WC}) \times (\frac{P_i \cdot \tau}{P_s \cdot N_d})} \times Q_E \tag{1}$$

where $Q_E$ represents the camera quantum efficiency, $F_{wc}$ is the camera full well capacity, $S_{pr}$ is the camera spectral response, $b_t$ is the camera bit depth, $P_i$ is the optical power incident onto the spectrometer, $\tau$ is the camera exposure time, $P_s$ is the pixel size (area), $N_d$ is the pixel number of the line detector, and $R_i$ is the ratio of the number of electrons detected by the CCD to the full well capacity of the detector per pixel. The numerator in the equation indicates the average number of electrons detected by the detector per pixel, and the denominator indicates the average number of electrons incident onto the detector per pixel [2].

**Table 1.** Design parameters for a reflective optics-based spectrometer

| **Item description** | **Surface#** | **Radius (mm)** | **Thickness (mm)** | **Semi-Diameter (mm)** | **Tilt angles (°)** | |
|---|---|---|---|---|---|---|
| | | | | | x | y |
| Fiber ($NA = 0.13$) | 0 | Infinity | 50.8 | | | |
| Reflective Collimator (RC12APC-P01, Thorlabs Inc.) | 1 | 11 | -120 | 11 | 90 | |
| Grating: 960 lines/mm | 2 | Infinity | -35 | width: 12.7<br>length: 12.7 | 23.9 | |
| Fold mirror (siliver coated) | 3 | Infinity | 85 | width: 6.5<br>length: 15 | -5 | |
| Concave mirror (siliver coated) | 4 | -256 | -128 | 25.4 | -24 | 2.1 |
| Linear CCD image plane | 5 | | | 14.8 | | |

The axial resolution of an SD-OCT system is depended on the center wavelength and the spectral bandwidth, which is usually measured experimentally as the axial point-spread function (PSF) in response to a partial mirror input (sample). The coherence length of the light source was 2.7 $\mu$m in air as specified in the datasheet by the manufacturer.

Both the optical resolution of the spectrometer optics and detector array resolution influence the spectral resolution and consequently the axial imaging range of an SD-OCT system. The maximum axial imaging range of an SD-OCT system is given by:

$$Z_{max} = \frac{\lambda_0^2}{4n \cdot \frac{\Delta\lambda}{N}} \tag{2}$$

where $N$ is the total number of illuminated pixels at the line scan detector. The spectral resolution $\delta\lambda$ represents the spectral range integrated over a single pixel [14,20]. Considering an ideal case of linear sampling in wavenumber space, for a given spectral bandwidth of the input light, covering all the pixels of the linear camera can maximize the ranging depth. However, practical ranging depth is limited by the depth dependent sensitivity falloff, which can be calculated using equation (3) [3, 21, 22]:

$$F(Z_i) = 10\log_{10}\left[\frac{\sin(pRZ_i)}{pRZ_i} \cdot \exp\left(-\frac{a^2R^2Z_i^2}{4\ln 2}\right)\right] \tag{3}$$

where $Z_i$ is the imaging depth within the range of $0 \sim Z_{max}$, and $p$ is the pixel size that affects the interferometric signal. $R$ is the reciprocal linear dispersion and is expressed as $R = \Delta k/p$, indicating the width of the spectrum in wavenumber at the focal plane. $\Delta k$ is the wavenumber range per pixel. $a$ is the full width at half maximum (FWHM) wavelength-dependent spot diameter. Therefore, the sensitivity fall-off is determined mainly by the spot size of a monochromatic beam and the pixel width of the detector [14, 23, 24].

## 3. Spectrometer Design

According to the above-mentioned design inputs, we propose to replace the refractive optics of the reference spectrometer: achromatic collimator (AC127-030-B, Thorlabs, USA) and camera lens (85 mm, $f/1.8D$, Nikon, USA) with reflective concave mirrors (Table 1). In the all-reflective optics spectrometer, the light exiting from the optical fiber was first collimated by a 90° off-axis reflective parabolic mirror, with a reflective focal length of 50.8 mm (RC12APC-P01, Thorlabs, Newton, New Jersey, USA) before dispersed by a grating. We used a planar mirror to fold the output of the grating and subsequently a concave mirror to focus the beam onto the linear camera (Fig. 1). In addition, considering different types of the light source (approximately Gaussian-shaped or rectangular-shaped light source) and the limited detector size, a proper diffraction grating with 960 lines/mm was used in the designed spectrometer system.

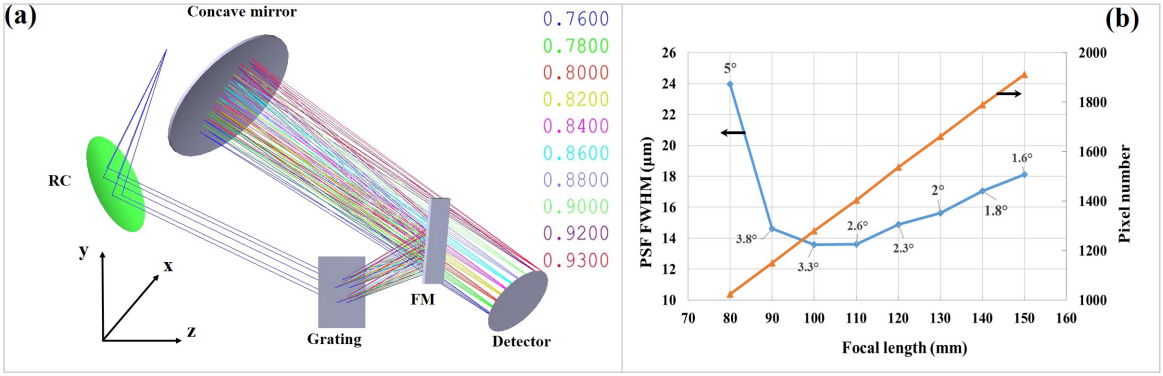


**Figure 1.** (a) Optical design for reflective optics-based spectrometer: Ray tracing of the designed spectrometer obtained using Zemax software. (b) The point-spread function (PSF) in the full width at half maximum (FWHM) and the covered pixel number for the spectrometer designs with different focal lengths.

There are multiple factors to consider during the design but we found the most significant two are the tilt angle and the focal length of the concave mirror after the grating. We designed a tilt angle of the concave mirror with respect to the center beam from the grating to avoid blocking the beam from the concave mirror to the detector by the folding mirror. However, this tilt angle gave rise to aberrations and consequently it will broaden the spot size. Although we could increase the focal length to reduce

the tilt angle and the corresponding aberration, it also resulted in increased spot sizes. In addition, with higher focal length, the total illuminated pixels' number is increased and therefore the imaging range is improved. Therefore, we had to make a compromise between focal length and the tilt angle to get the optimal sensitivity falloff. For the concave mirror with focal lengths of 80, 90, 100, 110, 120, 130, 140 and 150 mm, the minimized tilt angles evaluated using Zemax software are 5°, 3.8°, 3.3°, 2.6°, 2.3°, 2°, 1.8°, and 1.6°, respectively. We simulated the spot sizes (i.e., $a$)) and the covered pixel number (i.e., $N$) (Fig. 1(b)), using Zemax and the sensitivity fall-off curves based on the spot sizes in Fig. 1(b) using Eq. 3 (Fig. 2(a)). The pixel size ($p$) considered here was 14 $\mu$m as the pixel height of 28 $\mu$m only affects the total intensity of the signal [24]. According to our simulation results, there was a trade-off between the covered pixel number and the spot size. For our spectrometer design, we chose the best compromise: a focal length of 128 mm and tilt angle of 2.1°, to obtain the optimal 6-dB fall-off range up to 1.6 mm. We chose for our final spectrometer design. The optimized design parameters are listed in Table 1.

The detailed performance of the proposed design was characterized using spot diagrams and Huygens PSF cross sections (Fig. 2 (b)&(c)). The FWHM of Huygens PSF increases from 13 to 16 $\mu$m as the wavelength increases (Fig. 2(b)), which is similar in both of X and Y directions (Fig. 2(c)). Root mean square (RMS) radii of the spot diagrams are well within the Ariy disk, all of which demonstrate good focus quality. While it was not possible to obtain theoretical parameters for the sensitivity fall-off for a commonly used refractive optics-based spectrometer equipped with a commercial camera lens, as the optical configuration of the commercial camera lens is not available.

## 4. Experimental Verification

We constructed a high-resolution SD-OCT system and compared the performance of the proposed spectrometer with that of a typical refractive optics-based spectrometer (Fig. 3). A superluminescent diode (SLD) source with the output power of 8.8 mW was directed into a broadband 50:50 fiber coupler (TW850R5A2, Thorlabs, Newton, New Jersey, USA) which split the input light to the reference arm and the sample arm. Light backscattered from the sample interfered with light back-reflected from the reference arm, with half of the interference signal detected by the spectrometer. The refractive components in the reference and sample arms were identical. The reference arm included a polarization controller (PC), an achromatic collimation lens (L1) (AC080-010-B-ML, Thorlabs, Newton, New Jersey, USA), a focusing lens (L2) (AC127-020-B-ML, Thorlabs, Newton, New Jersey, USA), and a mirror, while in the sample arm, a pair of galvo scanner s(GVSM001/M, Thorlabs, Newton, New Jersey, USA) were used to scan the beam.

The refractive optics-based spectrometer (Fig. 3) consisted of an achromatic lens (AC127-030-B-ML, Thorlabs, Newton, New Jersey, USA), a transmission diffraction grating (1200 l/mm@840 nm, Wasatch Photonics, USA), a camera lens (85 mm,

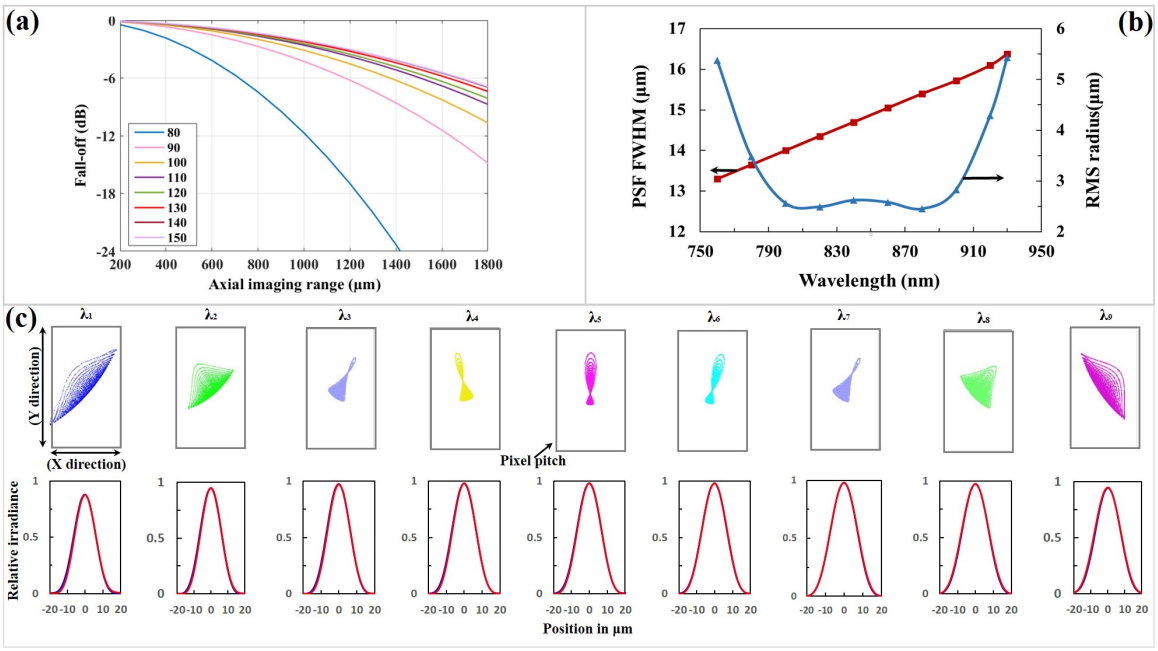


**Figure 2.** (a) The sensitivity falloff for the spectrometer designs with different focal lengths and optimal tilt angles. (b) The variation of the PSF FWHM (red, rectangle) and root mean square (RMS) radius (blue, triangle) with wavelength. (c) Spot diagram (top), and the cross-sectional PSF profile (bottom) for wavelengths of $\lambda_1 \sim \lambda_9$ (760-920 nm, 20 nm space) obtained using Zemax software. Black rectangles in the top figure demonstrates the pixel pitch (14 $\mu$m $\times$ 28 $\mu$m). Red and blue lines show cross section in the X and Y directions, respectively.

**Table 2.** Parameters for Spectrometer Efficiency Analysis

| Spectrometer Number | | Spectrometer Number | |
|---|---|---|---|
| $R_{refractive}$ | 0.313 | $R_{reflective}$ | 0.399 |
| $F_{WC}$ | $312500e^{-}$ | $S_{pr}$ | $120LSB/(nJ/cm^2)$ |
| $b_t$ | 12 | $\tau$ | $0.9 \star (1/20480)s$ |
| $Q_E$ | 0.5 | | |

f/1.8D, Nikon, USA), and the same line-scan detector. For reflective-optics based spectrometer, the diffraction grating was 960 lines/mm (Wasatch Photonics Inc.). The diffraction efficiency of the gratings of both spectrometers was similar. The interference signal was digitized with 12-bit resolution and then transferred to a computer via camera link cables and an image acquisition board (KBN-PCE-CL4-F, Bitflow, Woburn, Massachusetts, USA). The galvo scanners and the camera with maximum exposure time were synchronized by a triggering signal generated by the computer.

The performances of the reflective-optics based spectrometer were characterized by efficiency, axial ranging depth (6 dB fall-off), and axial resolution. The parameters used in Eq. (1) for spectrometer efficiency analysis are listed in Table 2. The experimentally measured efficiency for the refractive and reflective configurations was 0.336 and 0.428,

respectively, which agree very well with the theoretical values of 0.338 and 0.437 (the camera lens efficiency: 0.75 and grating efficiency: 0.9). Specifically, the efficiency of the proposed spectrometer is approximately 1.27 times higher than that of the refractive optics-based spectrometer (Fig. 4). This is because the efficiency of our customized concave mirror is approximately 25% higher than that of a typical camera lens for the wavelength range 760 nm to 930 nm. Note that within the wavelength range of 750-830 nm, the signal intensity of the reflective optics-based spectrometer is higher than that of the refractive-based system, which was caused by the field curvature introduced by the concave mirror.

Figure 5 shows that the 6-dB sensitivity fall-off ranges were $\sim 856\ \mu m$ and $\sim 943\ \mu m$ for the refractive and reflective optics based spectrometers, respectively. The number of pixels of the line-scan detector covered was 1569 and 1857 in the refractive optics based and reflective optics based spectrometers, respectively.

The axial resolutions of the refractive and reflective optics-based spectrometers were measured to be approximately 2.74 and 2.64 $\mu m$, respectively. The slightly improved axial resolution may be due to the elimination of chromatic aberrations. Therefore, the system performance shows improved efficiency when using the reflective optics-based spectrometer, with comparable ranging depth and axial resolution.

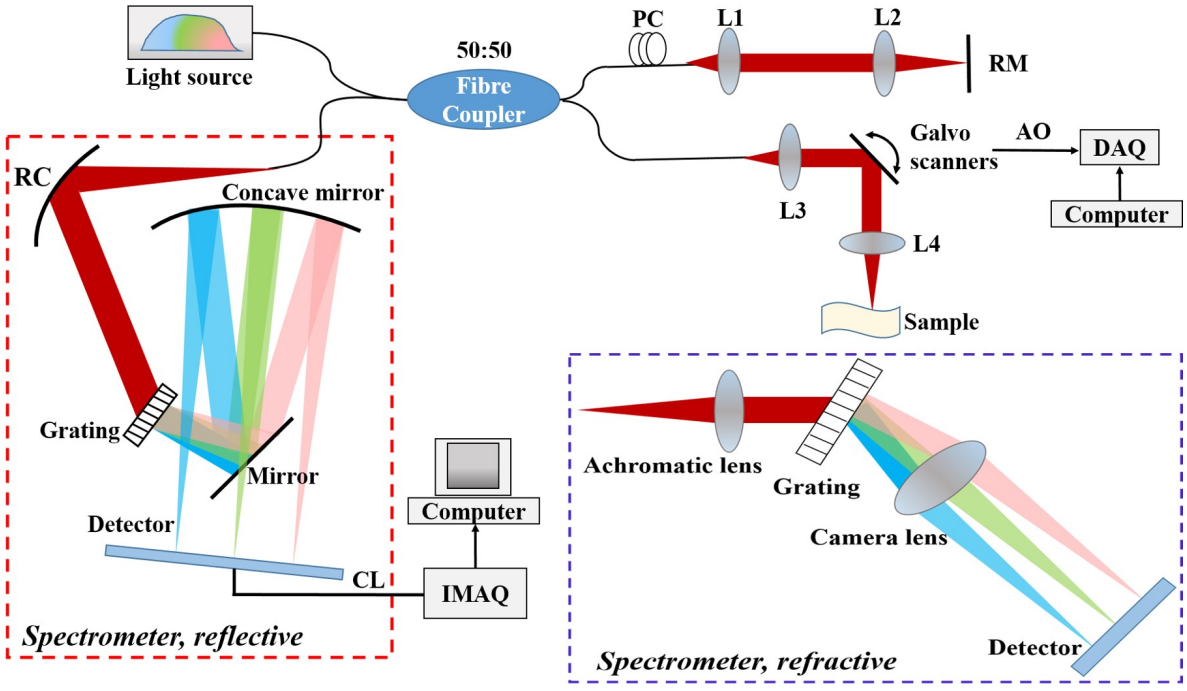


**Figure 3.** Experimental configuration of SD-OCT imaging system with the typically used refractive optics based and reflective optics based spectrometer. PC: polarizer controller; L1-L4: achromatic lens ; RM: reference mirror; AO: analog output; DAQ: data acquisition card; RC: reflective collimator; CL: camera link cable; IMAQ: image acquisition board.

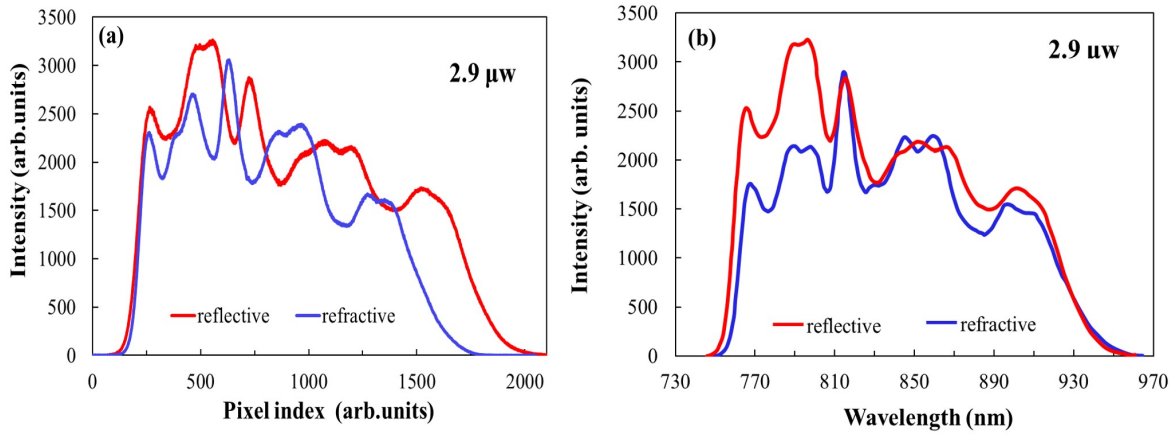


**Figure 4.** (a) intensity (arb. units) versus pixel index (arb. units) and (b) intensity (arb. units) versus wavelength. Refractive optics (blue) and reflective optics (red)-based spectrometer systems.

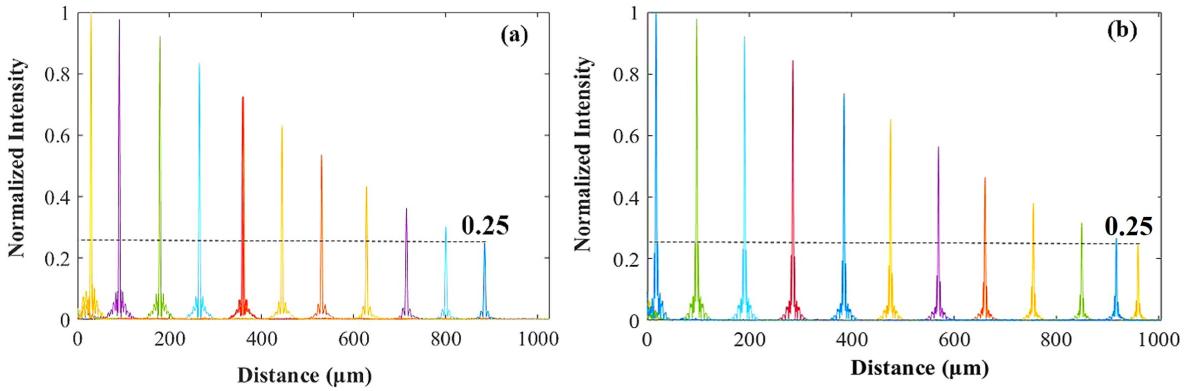


**Figure 5.** Depth profile of the imaged prism. (a) Refractive optics, and (b) reflective optics-based spectrometer for SD-OCT imaging system.

## 5. Discussions

The calculated and measured fall-off values at a ranging depth of approximately 1 mm are -2.5 dB and -6 dB, respectively. The difference is induced by unequal spectral bands in k-space integrated by the camera pixels in the experiment. The next step for our work is to improve the axial imaging fall-off by designing a linear-in-wavenumber spectrometer and then to use this instrument to image biological samples.

Although a comparable axial resolution was obtained in the current experiment, many clinical applications require cellular or sub-cellular resolution. Therefore, a broadband light source should be taken into consideration. For an SD-OCT system with an approximately Gaussian-shaped light source with 3dB wavelength range of 760-930 nm while the full range of 720-980 nm, cellular level imaging can be achieved successfully by using the proposed concave mirror based spectrometer with a focal length of 100 mm.

## 6. Conclusion

In this study, we report an all-reflective spectrometer design that supports an ultrahigh resolution SD-OCT system. Compared with the typical refractive optics-based spectrometer, the proposed spectrometer offers three main improvements: (1) improved efficiency, (2) elimination of chromatic aberrations, and (3) reduced cost. The efficiency of the proposed spectrometer is approximately 1.27 times that of a refractive optics-based spectrometer for an SD-OCT system, with comparable ranging depth and axial resolution.

## Acknowledgments

This research was supported in part by the National Natural Science Foundation of China (Grant No. 61705184), the Natural Science Basic Research Plan in Shaanxi Province of China (Grant No. 2018JQ6014), the National Research Foundation Singapore (NRF-CRP13-2014-05), National Medical Research Council Singapore (NMRC/CBRG/0036/2013), Ministry of Education Singapore (MOE2013-T2-2-107), NTU-AIT-MUV program in advanced biomedical imaging (NAM/15005), and the Fundamental Research Funds for the Central Universities (Grant No. G2018KY0308).

## References

[1] Fercher A F, Hitzenberger C K, Kamp G and El-Zaiat S Y 1995 *Optics communications* **117** 43–48
[2] Leitgeb R, Hitzenberger C and Fercher A F 2003 *Optics express* **11** 889–894
[3] Wojtkowski M, Srinivasan V J, Ko T H, Fujimoto J G, Kowalczyk A and Duker J S 2004 *Optics express* **12** 2404–2422
[4] Yun S, Tearney G, Bouma B, Park B and de Boer J F 2003 *Optics Express* **11** 3598–3604
[5] Liu L, Gardecki J A, Nadkarni S K, Toussaint J D, Yagi Y, Bouma B E and Tearney G J 2011 *Nature medicine* **17** 1010
[6] Shi W, Liu X, Wei C, Xu Z J, Sim S S, Liu L and Xu C 2015 *Nanoscale* **7** 17249–17253
[7] Wojtkowski M, Bajraszewski T, Targowski P and Kowalczyk A 2003 *Optics Letters* **28** 1745–7
[8] Chu K K, Unglert C, Ford T N, Cui D, Carruth R W, Singh K, Liu L, Birket S E, Solomon G M and Rowe S M 2016 *Biomedical Optics Express* **7** 2494–2505
[9] Chong S P, Zhang T, Kho A, Bernucci M T, Dubra A and Srinivasan V J 2018 *Biomedical Optics Express* **9** 1477
[10] Nassif N, Cense B, Park B, Pierce M, Yun S, Bouma B, Tearney G, Chen T and De Boer J 2004 *Optics express* **12** 367–376
[11] Drexler W, Morgner U, Ghanta R K, Kärtner F X, Schuman J S and Fujimoto J G 2001 *Nature Medicine* **7** 502
[12] Drexler W 2004 *Journal of Biomedical Optics* **9** 47–74
[13] Povazay B, Bizheva K, Unterhuber A, Hermann B, Sattmann H, Fercher A F, Drexler W, Apolonski A, Wadsworth W J and Knight J C 2002 *Optics Letters* **27** 1800–2
[14] Drexler W and Fujimoto J G 2008 *Optical coherence tomography: technology and applications* (Springer Science & Business Media)
[15] Yao X, Gan Y, Marboe C C and Hendon C P 2016 *Journal of biomedical optics* **21** 061006–061006
[16] Yuan W, Mavadia-Shukla J, Xi J, Liang W, Yu X, Yu S and Li X 2016 *Optics letters* **41** 250–253

[17] Liu L, Chu K K, Houser G H, Diephuis B J, Li Y, Wilsterman E J, Shastry S, Dierksen G, Birket S E, Mazur M *et al.* 2013 *PloS one* **8** e54473
[18] Yu X, Liu X, Chen S, Luo Y, Wang X and Liu L 2015 *Optics express* **23** 26399–26413
[19] Kamal M, Sivakumar N and Packirisamy M 2010 Design of a spectrometer for all-reflective optics-based line scan fourier domain optical coherence tomography *Photonics North 2010* vol 7750 (International Society for Optics and Photonics) p 775020
[20] Xi P, Mei K, Bräuler T, Zhou C and Ren Q 2011 *Applied optics* **50** 366–372
[21] Wang K, Ding Z, Wu T, Wang C, Meng J, Chen M and Xu L 2009 *Optics express* **17** 12121–12131
[22] Lan G and Li G 2017 *Scientific Reports* **7**
[23] Hu Z and Rollins A M 2007 *Optics letters* **32** 3525–3527
[24] Hu Z, Pan Y and Rollins A M 2007 *Applied optics* **46** 8499–8505